DOI 10.5162/ettc2018/7.3

Application of Fibre Bragg Grating Sensors to a Stalled High Lift Wing

Erica Alcusa-Saez, Stephen W. James, Simon Prince, Edmond Chehura, Nicholas J. Lawson and Ralph P. Tatam
School of Aerospace, Transport and Manufacturing, Cranfield University, Cranfield, MK43 0AL, UK
s.w.james@cranfield.ac.uk

Abstract
An array of optical fibre Bragg grating strain sensors attached to a high lift wing configuration in a low speed wind tunnel has been used to monitor successfully the steady flap deflection and the fluid shedding frequency generated by the flap. The shedding frequencies match closely those obtained previously using hot wire anemometry.

Key words: Optical fibre sensors, fibre Bragg gratings, shedding frequencies, high lift wing, flap deflection, wind tunnel.

Introduction

The aerofoils of unmanned aerial vehicles and small scale wind turbines often operate at low chord Reynolds numbers, making them prone to the development of a separated shear layer arising from boundary-layer separation. Depending on the Reynolds number and the angle of attack, this can lead to the formation of separation bubbles and vortex shedding, which negatively affect aerofoil performance [1] and can impart unsteady forces to the aerofoil, causing flutter. There has been interest in characterizing such flow features by measuring the surface pressure distribution along the span, determined using a number of pressure taps [1], and by monitoring the wake using hot wire anemometers and the structural vibration of the aerofoil using accelerometers [2].

Optical fibre sensors (OFS) are becoming viable replacements for traditional wind tunnel and flight test sensors. OFS systems capable of measuring geometry, strain, pressure and temperature - the main measurement variables of interest for basic aerodynamic analysis - are becoming well established in industrial sectors such as oil and gas and wind energy, and there is a long-standing interest in their use in wind tunnel and aircraft structural health monitoring [3-7] and wing shape measurement [8, 9].

The key benefits of OFS that drive this interest include their immunity to electromagnetic interference, the low weight of the sensor elements, the ability to embed optical fibres into composite materials or to surface mount, with a low profile, to metals, and the ability to perform multiplexed or distributed measurements within a single length of optical fibre.

The focus of this paper is on the use of optical fibre Bragg grating sensors (FBGs) to undertake measurements of the dynamic aerodynamic loading on a high lift wing in a wind tunnel in order to determine parameters of aerodynamic interest; the steady flap deflection and the shedding frequency.

Optical Fibre Bragg Gratings

An FBG consists of a periodic modulation of the refractive index of the core of an optical fibre, which reflects a specific wavelength the Bragg wavelength, back along the optical fibre, all other wavelengths pass thorugh the grating [10]. The Bragg wavelength, λ_B is dependent upon the period of the grating, Λ and the refractive index of the propagating mode, n_{eff}, according to

$$\lambda_B = 2n_{eff}\Lambda \qquad (1)$$

Typically, the refractive index modulation is introduced to the optical fibre by illuminating the fibre from the side with a spatially modulated UV laser beam [11]. The reflected Bragg wavelength is sensitive to perturbation of the grating structure by parameters such as strain and temperature. The measurement of the Bragg wavelength forms the basis of FBG sensing [12]. The strain sensivity of an FBG arises from a combination of the physical change in the period of the grating and the chnage in the refarctive index of the fibre via the elasto-optic effect

$$\Delta\lambda/\lambda_B = (1-p)\ \varepsilon \qquad (2)$$

Where p is the elasto-optic coefficient (0.22 for silica), ε the strain, and Δλ is the change in Bragg wavelength. For an FBG fabricated in standard telecomunications optical fibre (SMF28), the sensitivity is 1.2 pm/με.

A major advantage of FBG technology is that an array of uniquely identifiable sensors can be multiplexed within a single length of optical fibre by fabricating each FBG in the array with a different grating period, and thus a different Bragg wavelength at quiescent conditions [12]. While a number of approaches to the interrogation of FBG sensor arrays have been reported, the majorty of commercially available interrogation units employ a wavelength-swept laser to illuminate the sensors, and a photodiode to detect the reflected signals.

Experiment

5 FBGs were fabricated in a length of SMF-28 optical fibre that had been hydrogen loaded to increase its photosensitivity. The fibre was side-illuminated via a phase mask using the output at a wavelength of 266 nm from a frequency quadrupled flashlamp pumped Nd:YAG laser. A different phase mask was used for the fabrication of each FBG, such that, in their quiescent states, the FBGs were of different Bragg wavelengths, and thus could be multiplexed in the wavelength domain. Prior to exposure, the polyacrylate buffer jacket was removed from the sections of fibre into which the FBGs were to be written. Each FBG was of length 4 mm with a typical reflectivity of 50% and 3 dB bandwidth of 0.5 nm. The sections of optical fibre containing the FBGs were not subsequently recoated.

The 2D, 3 element high lift wing configuration, comprising a single slotted leading edge slat, a main element and a single slotted trailing edge flap is shown schematically in Figure 1.

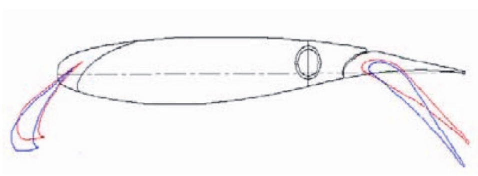

Fig 1. 2D 3 element high lift wing

The wing has a stowed chord of 0.6 m and a span of 1.4 m. The FBG sensors were bonded to the surface of the trailing edge flap, having chord length of 180 mm, oriented along the spanwise direction, 140 mm from the trailing edge, using cyanoacrylate adhesive. The physical arrangement of the FBGs is illustrated in Fig. 2, where FBG 3 was positioned at the mid-point of the span of the slat. The fibre was terminated with an FC/APC connector to allow connection to the FBG interrogator.

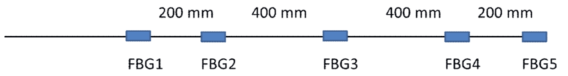

Fig. 2. Arrangement of FBG sensor array

The FBG sensor array was interrogated using a SmartScan Aero Interrogator (Smart Fibres, UK). The interrogator has a data rate of 2.5 kHz, a wavelength scan of 40 nm, a resolution of 1pm and can monitor 16 wavelength division multiplexed FBGs in a single optical fibre . The interrogator can be used to monitor up to 4 fibres simultaneously.

The wing was suspended between two 1.2 m diameter circular end plates, as is shown in Figure 3, to facilitate its mounting vertically in an 8x6 foot wind-tunnel such that its angle of attack was adjustable. The wind speed could be changed from 0 m/s to a maximum of 42 m/s.

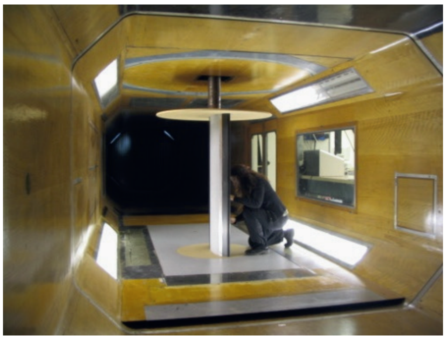

Fig. 3. The 2D 3 element high lift wing mounted in a 8x6 foot wind-tunnel

Wing angles of attack in the range 0^o to 20^o were selected to initiate a stall characteristic off the flap section, allowing the use of the FBGs to detect the excitation of the slat at the fluid shedding frequencies. For each angle of attack the wind speed was varied from 16 m/s to 40 m/s, giving a Reynolds number range based on flap chord of 195,000 to 488,000. The signals from the FBGs were acquired over a duration of 10s at each wind speed and subsequently filtered to reduce the noise. The frequency content of the strain data was calculated using a fast Fourier transform.

Results and Discussion

Figures 3(a) and (b) show the changes in load experienced by the slat at the locations of the 5 FBG sensors at two angles of attack; 0^o and 20^o as the wind speed was increased from 0 to 40 m/s, held at 40 m/s and subsequently reduced to 0 m/s. This illustrates the ability of the sensors to monitor the steady flap deflection. The distribution of the strain shows that for the steady measurement the strain is largest at center of the slat, and the loads are larger for high angles of attack. This is consistent with an aerofoil up to a stall condition.

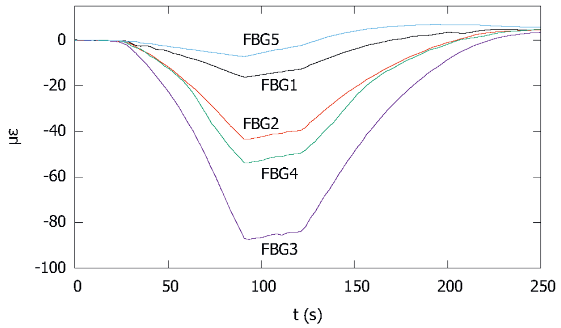

(a)

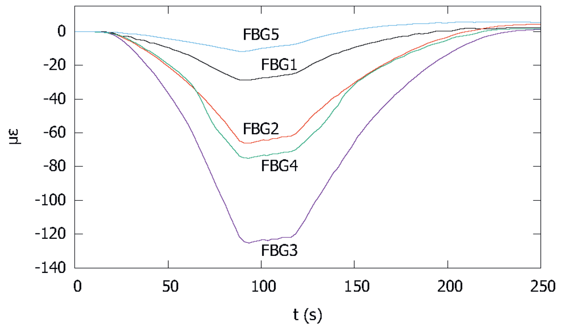

(b)

Fig. 3. Strain measured by the FBG sensors with increasing wind speed, at angles of attack (a) 0^o and (b) 20^o

Fig. 4 shows the power spectra of the signals obtained from FBG 3 for an angle of attack of 20^o at three wind speeds, 16 m/s, 20 m/s and 24 m/s. Each spectrum exhibits a dominant frequency, which increases with increasing wind speed.

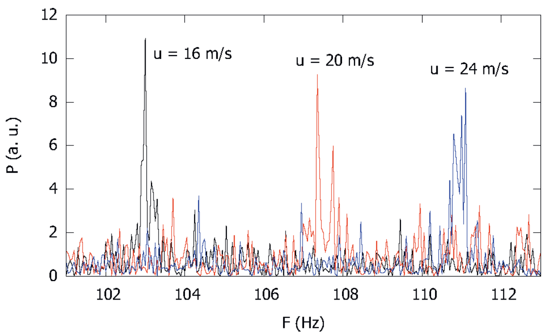

Fig. 4. Power spectrum of the strain data obtained from FBG 3 with increasing wind speed (u), at an angle of attack 20^o.

Figures 5 (a) and (b) show the variations in the shedding frequency with wind speed for 0^o and 20^o angles of attack. The frequency shows a sigmoidal dependence upon wind speed, and the frequency increases with increasing angle of attack. This is consistent with previous reports [1,2]. The amplitude of the frequency component was dependent upon the location of the sensor (data not shown here), suggesting that the FBGs were sampling the vibration mode shape in the span-wise direction. This is the subject of further investigation.

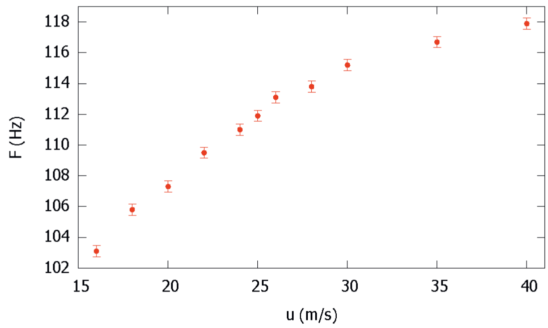

(a)

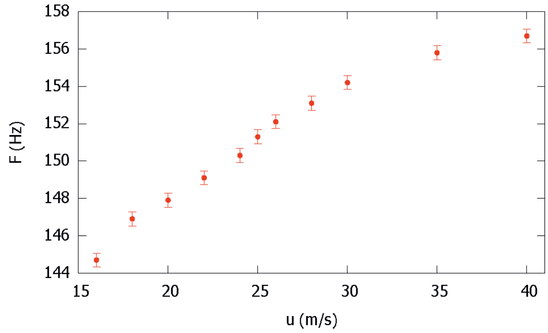

(b)

Fig.5. Variation in shedding frequency (f) plotted as a function of wind speed (u) for angles of attack (a) 0^o and (b) 20^o

From Figure 5, if the Stouhal number (St) is calculated based on flap chord, it is equivalent to St in the range 0.1 – 0.5. This compares with previous work on aerofoils with a similar Reynolds number range [1,2], where reported Strouhal numbers were in the range 0.15 – 0.25.. The higher upper limit of the Strouhal number measured in the present tests, which occur at the lower wind speeds at the highest angle of attack, is thought to be due to separations on the main element and possibly high frequency oscillations of a separation bubble on the flap. A second set of tests together with a study using high resolution computational fluid dynamics aims to shed more detail on this complex flow physics.

Summary

An array of five FBGs sensors was bonded to the slat of a high lift wing configuration, and used to monitor the static and dynamic loads experienced by the slat when the wing was subject to wind speed of 0 – 40 m/s in a low speed wind tunnel. The FBGs were able to detect the excitation of the flap at the fluid shedding frequencies characteristic of the aerofoil stall at angles of attack between 0^o and 20^o. Shedding Strouhal numbers were consistent with those reported in the literature for flows at similar Reynolds number, but more study is needed to properly interpret these results.

Thus, the preliminary results presented here show that the FBG system has successfully detected both the steady flap deflection and the associated shedding frequency in a stall, with dominant spectral frequencies ranging from around 100Hz to 160Hz, which closely matches expected frequencies reported from previous hot wire anemometry data.

References

[1] Yarusevych S and Boutilier M S H, Vortex Shedding of an Airfoil at Low Reynolds Numbers *AIAA J.*, 49, 2221 – 2227 (2011);doi: 10.2514/1.J051028.

[2] Zaman K, McKinzie D J and Rumsey C L, A natural low-frequency oscillation of the flow over an airfoil near stalling conditions, *J . Fluid Mech*. 202, 403-442 (1989); doi: 10.1017/S0022112089001230

[3] Read I J and Foote P D Sea, and flight trials of optical fibre Bragg grating strain sensing systems *Smart Mater.Struct.* 10, 1085–94 (2001); doi: 10.1088/0964-1726/10/5/325

[4] Lee J-R, Ryu C-Y, Koo B-Y, Kang S-G, Hong C-S and Kim C-G, In-flight health monitoring of a subscale wing using a fiber Bragg grating sensor system *Smart Mater. Struct.* 12 147–155 (2003); doi: 10.1088/0964-1726/12/1/317

[5] Papageorgiou A W, Karas A R, Hansen K L, Arkwright J W, Monitoring pressure profiles across an airfoil with a fiber Bragg grating sensor array, *Proc. SPIE*, 10539, 105390C (2018); doi: 10.1117/12.2288024

[6] Singh D B and Suryanarayana G K Application of Fiber Bragg Grating Sensors for Dynamic Tests in Wind Tunnels, J. Indian Institute of Sci., 96, 47-52 (2016).

[7] Correia R, Staines S E, James S W, Lawson N, Garry K and Tatam R P Wind tunnel unsteady pressure measurements using a differential optical fiber Fabry-Perot pressure sensor, *Proc. SPIE* 9157, 915708 (2014); doi: 10.1117/12.2059631

[8] Lawson N J, Correia R, James S W, Partridge M, Staines S E, Gautrey J E, Garry K P, Holt J C and Tatam R P Development and application of optical fibre strain and pressure sensors for in-flight measurements, Meas.Sci.Technol. 27, 104001 (2016); doi: 10.1088/0957-0233/27/10/104001/.

[9] Ko W L, Richards W L and Fleischer V T, Applications of Ko displacement theory to the deformed shape predictions of doubly tapered ikhana wing NASA/TP-2009-214652 (2009).

[10] Jutte C V, Ko W L, Stephens C A, Bakalyar J A, Richards W L and Parker A R Deformed shape calculation of a full-scale wing using fiber optic strain data from a ground loads test NASA/TP-2011-215975 (2011).

[11] Kashyap R, Fibre Bragg Gratings (2nd Edition) Academic Press (2009).

[12] Bennion I, Williams J A R, Zhang L, Sugden K and Doran N J, UV-written in-fibre Bragg gratings Opt Quant Electron 28, 93-135 (1996); doi: 10.1007/BF00278281.

[13] Othonos A, Fiber Bragg gratings, Rev. Sci. Instrum. 68, 4309 (1997); doi:10.1063/1.1148392